Ultrastructure of the Human Aortic Fibrolipid Lesion

Formation of the Atherosclerotic Lipid-Rich Core

THOMAS M. A. BOCAN, PhD,
THOMAS A. SCHIFANI, and JOHN R. GUYTON, MD

From the Department of Medicine and Cell Biology, Baylor College of Medicine, Houston, Texas

The formation of the atherosclerotic lipid-rich core has been elucidated by electron microscopy of the core region in small, raised fibrolipid lesions. The relationship among lipid deposits, extracellular matrix, and cells found in distinct regions of the fibrolipid lesion was examined. Extracellular lipid droplets, verified by osmium-thiocarbohydrazide-osmium staining, made up approximately 40% of the lipid-rich core volume. The lipid droplets were often found distinctly associated with elastin and/or collagen; these associations were dependent upon the location examined within or near the lipid-rich core. Within areas of intense extracellular lipid deposits, crystalline clefts suggesting cholesterol monohydrate were observed. Stereologic analysis of the lipid-rich core components revealed marked reductions in the volume fractions of cells, reticular ground substance, and basement membrane; while the extent of extracellular lipid increased 7–10-fold. Eleven percent or less of lipid in the core region was found within cells, usually smooth muscle cells. Above the core region in the lesion cap, monocyte-macrophage foam cells were prominent. Cellular lipid droplets were much larger (profile diameters sixfold higher) than extracellular droplets. With these data as well as transitional morphologic features at the boundaries of the core region, it is suggested that 1) the abundant extracellular lipid does not derive from cell necrosis, and 2) lipid deposition in association with extracellular matrix constituents is an early event in the development of the lipid-rich core. (Am J Pathol 1986, 123:413–424)

WE HAVE reported that precursor lesions of the atherosclerotic fibrous plaque can be identified consistently within the human aorta.[1] These raised lesions, termed "fibrolipid lesions," covered less than 16 sq mm of surface area and possessed total intimal volumes ranging from 3 to 43 μl, with the majority less than 16 μl. Light-microscopic examination of fresh-frozen sections of these lesions characteristically showed superficial clusters of foam cells and a deeper lipid-rich core. The lipid-rich core appeared to originate near the inner limiting elastic membrane, which marks the boundary between the elastic hyperplastic (middle) and musculoelastic (deepest) intimal layers. In tissue sections stained with oil red O, the lipid-rich core appeared to contain predominantly extracellular lipid. Cholesterol crystals, identified by polarizing light microscopy, were found in 37% of the lesions. The location of the fibrolipid lesion at sites of predilection for fibrous plaque development, the relationship to subject age, the presence of a lipid-rich core with cholesterol monohydrate crystals, and a chemical composition comparable to fibrous plaques strongly suggested that the fibrolipid lesion was a precursor to the fibrous plaque. Reported here is an ultrastructural study of the same specimens of fibrolipid lesions examined earlier at the light-microscopic and chemical levels.

Most electron-microscopic studies of human atherosclerosis have focused on lesions at either end of the disease spectrum. Several investigators[2–4] examining fatty streaks have speculated that the lipid-rich core region of the fibrous plaque could develop from these lesions as a result of foam cell necrosis with release of the cellular lipid content into the extracellular space. However, scant evidence has been provided to suggest that this mechanism actually accounts for the bulk of core lipid accumulation. Smith et al[5] have suggested an

Supported by NIH Grant HL-29680, a grant from the American Heart Association (Texas affiliate), and a gift from Mr. and Mrs. Lev H. Prichard III. Dr. Bocan was supported by NIH Fellowship HL-07090 and NIH Training Grant HL-07282.

Accepted for publication January 15, 1986.

Address reprint requests to John R. Guyton, MD, Department of Medicine, A-601, The Methodist Hospital, 6565 Fannin Street, Houston, TX 77030.

alternative mechanism to foam cell degeneration. In normal intima, Smith and colleagues have found extracellular lipid deposition, termed "perifibrous lipid," even in the absence of foam cells. Our recent ultrastructural observations in normal aortic intima demonstrated that perifibrous lipid is localized preferentially to elastin fibers.[6] Thus, direct deposition of lipid in association with the extracellular matrix is an alternative hypothesis for lipid-rich core formation.

At the other end of the lesion spectrum, Ross and co-workers[7] have examined advanced lesions of the superficial femoral artery. They observed a relatively small amount of lipid in the lesions. After examining the growth characteristics of the smooth muscle cells isolated from these lesions, they suggested that these cells had senesced. It seems likely that the lesions examined were beyond the period of relatively rapid growth. By focusing on apparently progressive lesions, more advanced than fatty streaks but not yet to the stage of senescent fibrous plaques, we may gain insight into the role of cellular degeneration in lipid deposition and/or possibly the role of the extracellular matrix constituents in lipid-rich core formation.

Thus the present study aimed to describe the ultrastructural appearance of the fibrolipid lesion, a precursor of the atherosclerotic fibrous plaque. Special attention was given to the relationship among cells, extracellular matrix, and lipid deposition found in distinct regions of the fibrolipid lesion, ie, cap, lipid-rich core, and core periphery. We performed a stereologic analysis of lesion connective tissue elements and lipid in order to ascertain whether any significant changes in the extracellular matrix of the core occurred with lesion initiation and development. Core region development via lipid deposition within the extracellular matrix was strongly suggested by 1) discrepancies between the sizes of cellular and extracellular lipid droplets and 2) consideration of the transitional morphologic findings observed at the boundaries between core region and adjoining tissue.

Materials and Methods

Selection of Fibrolipid Lesions

The material examined here by electron microscopy consisted of intervening slices from our previously reported light-microscopic and chemical analysis of fibrolipid lesions.[1] The lesions were found in 147 aortas (132 from men, 15 from women) obtained at autopsy. The aortas were from individuals aged 18–71, with 85% of the individuals aged 45 or younger. Trauma was the cause of death in about 90% of the cases. All distinct raised lesions covering no more than 16 sq mm surface area were dissected from the descending thoracic and abdominal aorta. The small raised lesions, when viewed from above, were covered by either a cluster of small yellow dots, a homogeneous yellowish cover, fingerlike projections of a white fibrous material, or a complete pearly white cap. Lesions were sliced transversely at 1-mm intervals with the aid of a McIlwain Mechanical Tissue Chopper (Mickle Laboratory, Brinkmann Instruments, Westbury, NY). About three-fourths of the small raised lesions contained lipid deposits fluorescing yellow-orange under ultraviolet light and stainable with oil red O. The lipid-containing lesions, termed "fibrolipid lesions," constituted the primary tissue material for our previous studies and for the electron-microscopic studies reported here.

Tissue Processing for Electron Microscopy

Selected tissue slices were transected at the site of maximum intimal thickness. The two halves from each lesion were fixed in 2% paraformaldehyde and 2.5% glutaraldehyde in 0.13 M sodium phosphate buffer, pH 7.4, for 24 hours at 4 C. After an overnight buffer wash, the tissues were postfixed in 2% aqueous osmium tetroxide, stained *en bloc* with 1% uranyl acetate in 0.05 M sodium maleate buffer, pH 6.0, dehydrated through a graded ethanol series (to 100% ethanol over 2–3 hours at 25 C) and in propylene oxide, and embedded in Epon 812. Representative slices of normal intima were processed along with the fibrolipid lesions. Gold to silver–gold thin sections were cut on an LKB III Ultratome and stained with 3% uranyl acetate in 30% ethanol and Reynolds lead citrate sequentially.

A selected group of lesions were also fixed in 3% glutaraldehyde in 0.1 M cacodylate buffer, pH 7.2, for 24 hours at 4 C. These lesion slices were subsequently stained with an osmium-thiocarbohydrazide-osmium (OTO) sequence *en bloc* as described by Willingham and Rutherford[8] and Guyton et al.[6] The OTO procedure was used for increased preservation and high-contrast positive staining of lipid-containing structures. This procedure entailed incubating 200-μ lesion slices in 1.5% OsO_4 in 0.1 M cacodylate buffer, pH 7.4, for 30 minutes followed by 1% thiocarbohydrazide in H_2O for 5 minutes, then 1.5% OsO_4 for 30 minutes. Extensive washing of lesion slices with 0.1 M cacodylate buffer, pH 7.4, was performed between each step. The thiocarbohydrazide solution used was freshly prepared each day by adding solid thiocarbohydrazide to H_2O at 58 C with intermittent shaking for 3–4 hours. The solution was cooled to room temperature and filtered through a 0.22-μ Millipore fiilter. After staining, the

lesion slices were dehydrated at 4 C in a graded series of acetone to 100% acetone over 1 hour, infiltrated with the use of 1:1 acetone/Epon 812 overnight at 4 C, and embedded in Epon 812. Thin sections were examined without additional staining.

Selection of Electron Micrographs

Two-micrometer plastic sections were cut from each of the tissue block faces prior to ultrathin sectioning. After staining with toluidine blue–basic fuchsin, the lipid-rich core could be distinguished from the surrounding intima on the basis of the core's intense negative metachromasia, which gave it a greenish hue. The surrounding tissue was magenta to blue in color. The tissue block was trimmed to include the lipid-rich core and core periphery. Ultrathin sections were then cut from 27 different fibrolipid lesions, stained, and examined on a Phillips 201 transmission electron microscope. For some lesions, the tissue block containing the opposing face of the lesion was trimmed so as to examine the more superficial layers, which would include the lesion cap above the lipid-rich core.

Electron microscopy of the lesions included qualitative and quantitative approaches. For stereologic assessment of the lipid-rich core, 12 of the 27 lesions were randomly selected and the areas to be photographed were selected in an unbiased manner. At a magnification of 1000× the lipid-rich core was located and the center determined with the microscope stage micrometers. The magnification was increased to 7000×. Again using the stage micrometers, three micrographs were photographed at the corners of an equilateral triangle, the sides of which were one-quarter the average diameter of the entire core region. A triangle of this size was chosen so as to obtain an unbiased sampling at three separate, nonoverlapping sites around the center of the lipid-rich core. Micrographs of normal intima were selected in a manner described previously[6] from subjects matched for age, race, and sex. This simply entailed obtaining micrographs 50 μ above and 50 μ below the inner limiting elastic membrane (ILM). It was determined from light-microscopic observations that the lipid-rich core of the fibrolipid lesion and the deposition of extracellular lipid (perifibrous) in normal intima were both characteristically found about the ILM. Although not all lipid-rich cores of the fibrolipid lesion were located exclusively along the ILM, most of the core regions were found in the elastic hyperplastic layer above the ILM or in the musculoelastic layer just below the ILM. Thus, the 100 μ about the ILM was useful in determining what the volume composition of normal intima was at the predominant site of the lipid-rich core. Each micrograph was printed at a final magnification of 19,600× for stereologic analysis. Component volume fractions were determined with the use of a point grid overlay of approximately 150 points.

Stereologic Analysis

The criteria established to identify structures for stereologic analysis were as follows. Fibrillar collagen consisted of bundles of fibrils with axial periodicity. Elastin consisted of a fibrillar substance containing moderate numbers of electron-dense microfibrils or a pale electron-lucent material of glassy appearance, more dense than the surrounding reticular space, lacking periodicity and containing a few dense microfibrils. Basement membrane was identified as a homogeneous electron-dense layer or multilayered structure in close association with cells. Reticular ground substance was characterized as an electron-lucent space superimposed by a reticular pattern of fibrils and granules, which represent matrix proteoglycans. Lipid droplets both intracellular and extracellular were identified as vesicular structures, often containing a thick crescent of an electron-dense material surrounding a clear center. Some of the cellular droplets were identifiied as solid osmiophilic round structures. Vesicles without a crescent of osmiophilic material were also categorized as lipid droplets with the central lipid completely removed in processing. Since it was sometimes difficult to distinguish between smooth muscle cells and monocyte-macrophages, the volume fraction of all cells in normal intima and lipid-rich core was determined. The volume fraction of the various components was tabulated for normal intima and the fibrolipid lesions with and without cholesterol crystals. These categories of fibrolipid lesions were based on previous results using polarizing light microscopy.[1] Statistical comparisons of the volume fraction was performed using analysis of variance. The P value was corrected for multiple comparisons by Bonferroni's method.[9]

The diameters of cellular and extracellular lipid droplet profiles were also determined on the micrographs of the lipid-rich core. For elliptical droplet profiles, the length of a chord bisecting the angle of the major and minor axes was recorded as the profile diameter. A total of 300 intracellular and 300 extracellular droplet profiles were measured. A point grid overlay was used for random selection of extracellular droplet profiles for measurement. Thus, the likelihood of recording the diameter of a given droplet profile was proportional to the area of that droplet profile. The sizes of all osmiophilic droplets within cells were measured, since cells with lipid droplets were infrequent in the micrographs

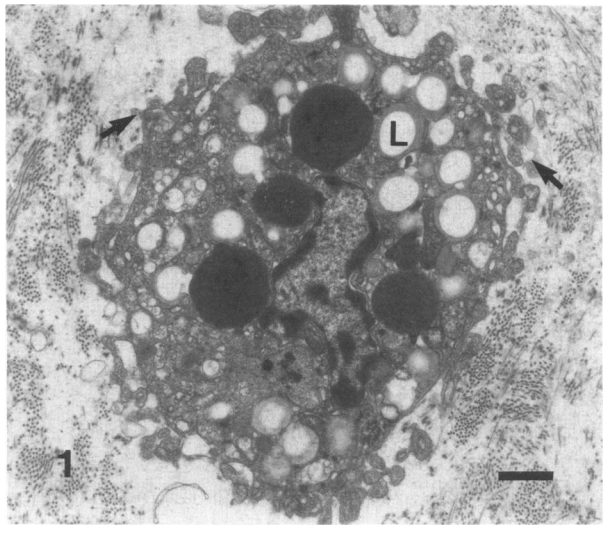

Figure 1—Lipid droplets within a monocyte-macrophage in a lesion cap. The lipid droplets (*L*) contain a rim of osmiophilic material. The cell possesses prominent micropodia (*arrows*) and lacks a surrounding basement membrane. The loose arrangement of collagen and reticular ground substance, without extracellular lipid, is typical of the appearance of the lesion cap. (Uranyl acetate and lead citrate, bar = 1 μ, ×8100)

examined. Since all cellular droplets were measured, a correction was necessary for an accurate comparison of cellular and extracellular droplet diameters. The cellular lipid distribution was corrected by multiplying the number of droplets at each interval by the square of the profile diameter (proportional to profile area). This allowed for an accurate representation of the area fraction of lipid contained in droplet profiles of each size category.

Results

Qualitative Observations

Lesion Cap

The lesion cap contained collagen bundles, reticular ground substance and scant elastin fibers. Visible lipid was almost entirely cellular; extracellular lipid droplets were rarely found. Monocyte-macrophage foam cells (Figure 1), smooth muscle cells (SMCs) with and without lipid inclusions, infrequent macrophages with few or no lipid inclusions, and infrequent lymphocytes were found in this area of the fibrolipid lesion.

Lipid-Rich Core Region

The lipid-rich core of the fibrolipid lesion was characterized by abundant extracellular lipid (Figure 2). Lipid-rich cores were found in the deep intimal layers; ie, the musculoelastic layer adjacent to the internal elastic lamina and in the more superficial elastic hyperplastic layer. Cholesterol crystals were sometimes found within these regions of dense extracellular lipid deposition (Figure 3). In several of the larger fibrolipid lesions calcific spheroids (Figure 4) could be observed scattered in the extracellular space. These structures corresponded to the eosinophilic spheroids, positive for calcium by von Kossa staining, noted earlier by light microscopy.[1] Ultrastructurally, the calcific spheroid appeared as a circle with a very electron-dense periphery surrounding a clear or reticular core. SMCs of several distinct appearances were present within the lipid-rich core; however, the number of cells was much less than that observed at the periphery of the core. The SMCs were surrounded by a basement membrane and intact plasma membrane with distinct micropinocytotic vesicles. SMC-derived foam cells with varying amounts of myofilaments and lipid inclusions were observed. SMCs with an extensive rough endoplasmic reticulum and abundant free and attached ribosomes were also present. Flattened SMCs within collagen bundles and stellate SMCs associated with elastin fibers were present in the lesions; however, they were infrequent within the core region.

The lipid droplets which comprised approximately 40% of the lipid-rich core volume had several appearances. Often the lipid droplets were seen as vesicular structures with an enclosed crescent of an electron-dense material surrounding a clear center (Figure 2a). Vesicles, presumed to be lipid droplets, without a crescent of osmiophilic material, were also observed in regions of a dense, finely granular matrix possibly representing elastin (Figure 3a). Cellular lipid droplets were similar in appearance to the extracellular droplets. However, the droplets were much larger, and their osmiophilic centers were retained better through the course of tissue preparation (Figure 1). In a few apparently necrotic cells, these droplets showed a scalloped or "cut-out" contour to the droplet border. Scalloping of extracellular droplets was not evident in the tissue specimens processed for electron microscopy in a routine manner. In the fibrolipid lesion specimens stained

Figure 2—Lipid-rich core regions. **a**—A lipid-rich core developing in the musculoelastic layer of the intima. Lipid droplets (*arrows*) are present in elastin (*E*) and collagen (*C*). The electron-dense material adjacent to the elastin band has the appearance of immature elastin. An SMC is at the left. (×11,250) **b**—A lipid-rich core of the elastic hyperplastic layer. Lipid droplets are located in prominent collagen bundles (*C*). Elongated SMCs surround the collagen. Elastin is relatively scant in this layer. (Uranyl acetate and lead citrate, bar = 1 μ, ×8325)

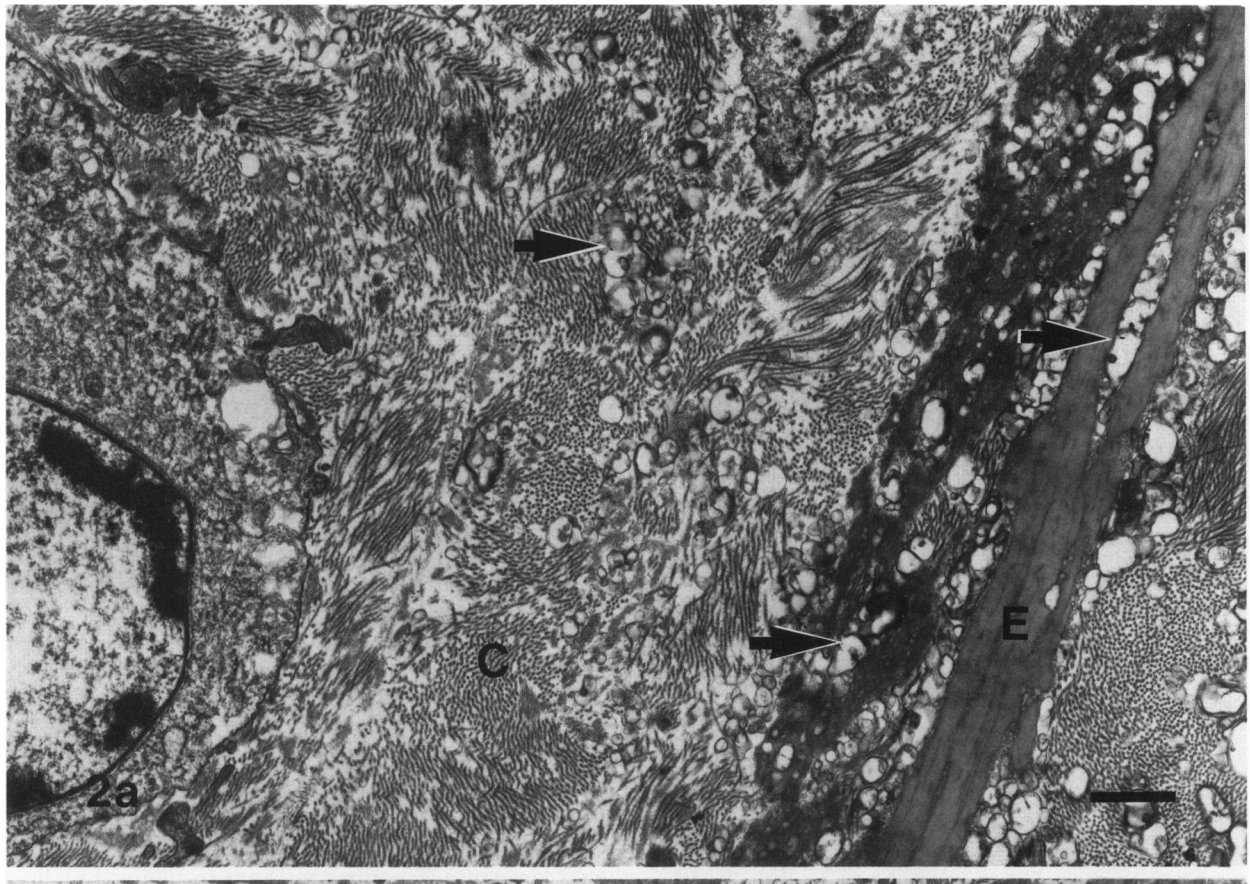
C
E
2a

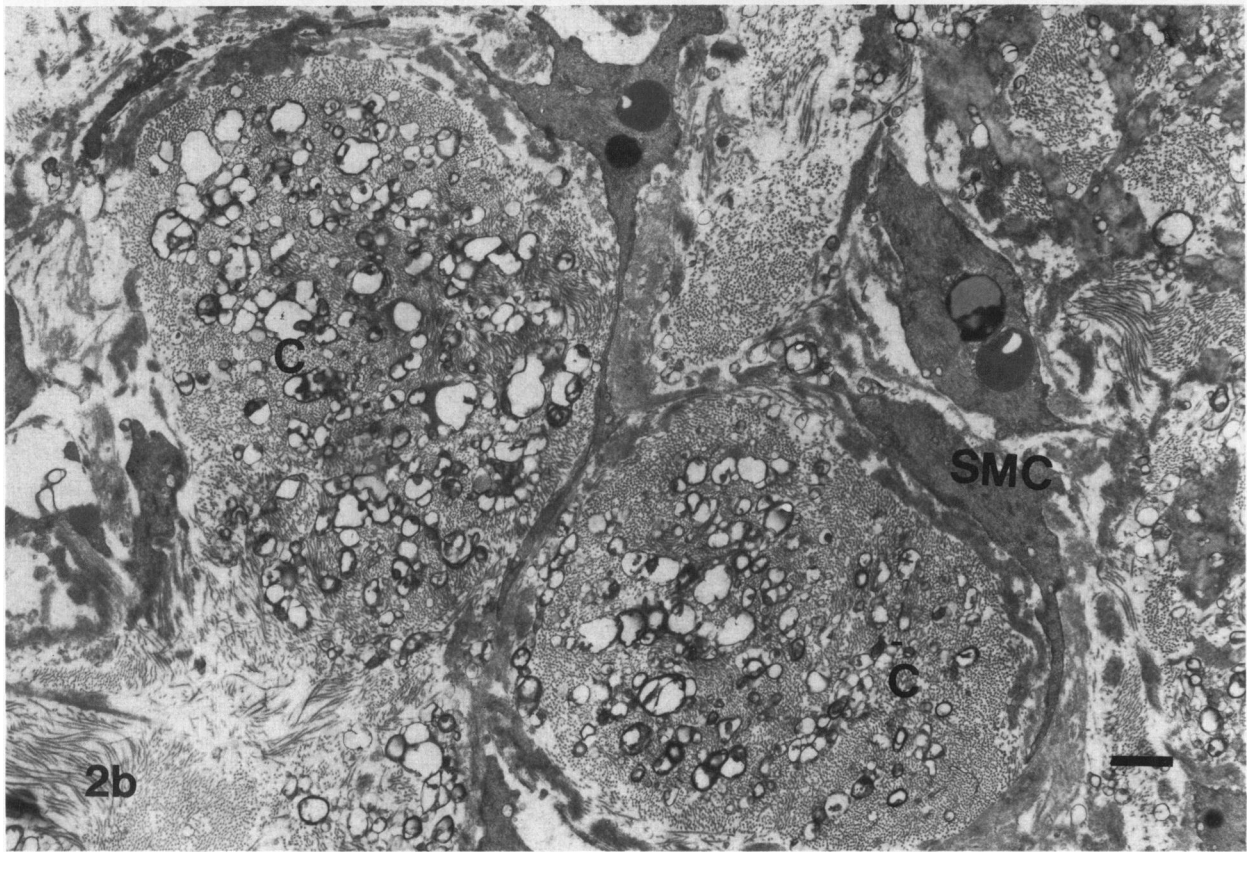
C
SMC
C
2b

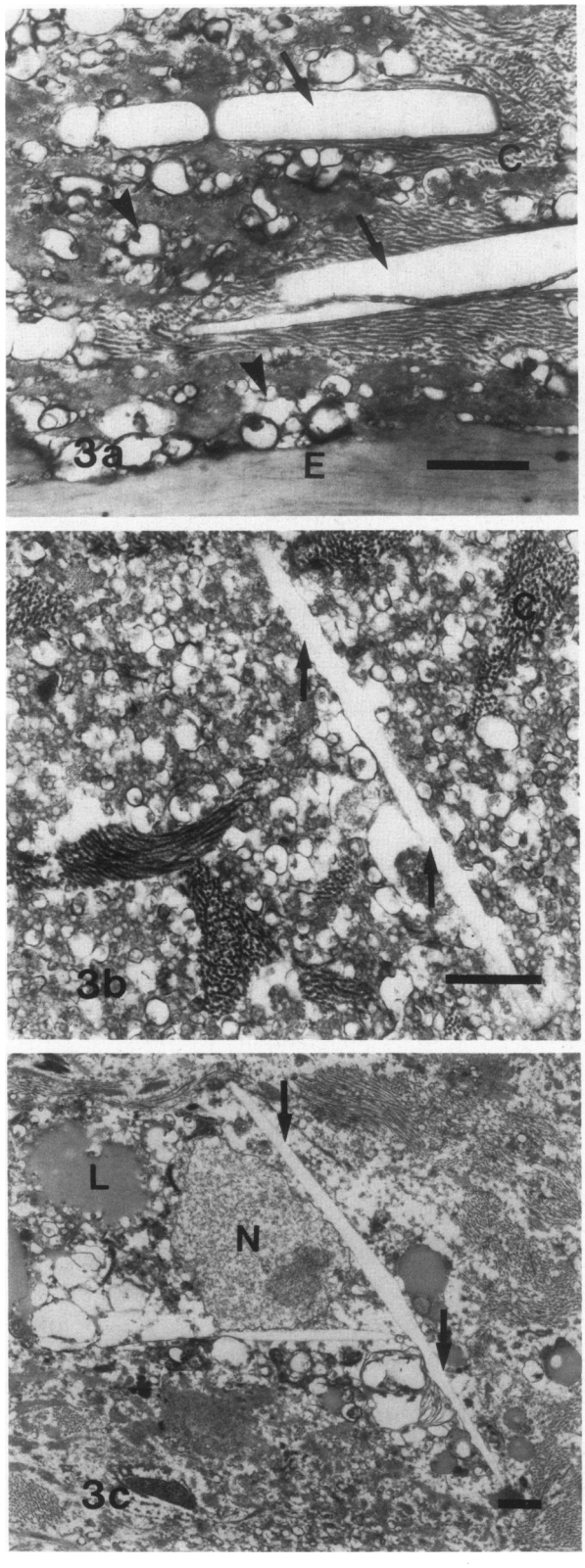

Figure 3—Cholesterol crystallization within the lipid-rich core. **a**—Cholesterol clefts (*arrows*) in close association with collagen (*C*) elastin (*E*) and an electron-dense material with the appearance of immature elastin. Extracellular lipid droplets (*arrowheads*). (×15,000) **b**—Cholesterol clefts (*arrows*) in an area of small vesicles surrounded by a granular matrix. *C*, collagen. (×14,175) **c**—Cholesterol clefts in an area of a necrotic cell. Note the remnant of a nucleus (*N*) and the scalloped appearance of the lipid droplet (*L*). Small extracellular lipid droplets are also present at the bottom of micrograph. (Uranyl acetate and lead citrate, bars = 1 μ, ×6300)

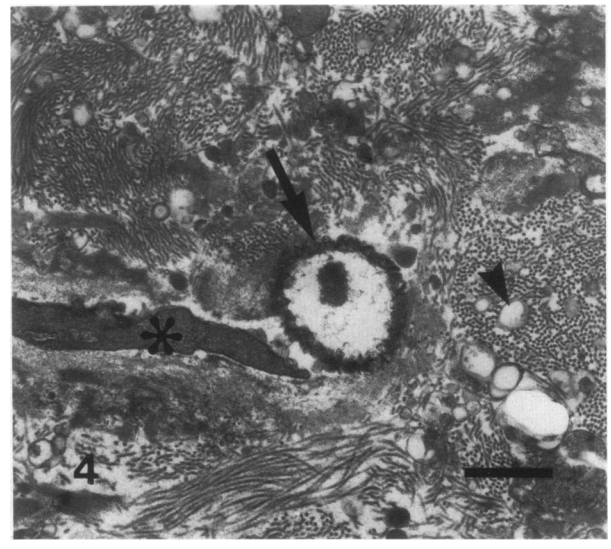

Figure 4—Calcific spheroid (*arrow*) associated with a flattened SMC (*asterisk*) amidst collagen and extracellular lipid deposition (*arrowhead*). (Uranyl acetate and lead citrate, bar = 1 μ, ×12,375)

with the osmium-thiocarbohydrazide-osmium (OTO) sequence, numerous extracellular lipid droplets showed a scalloped or cut-out contour (Figure 5). In the OTO-treated specimens, the extracellular and cellular lipid droplets were more pronounced and appeared as very electron-dense structures resistant to removal by lipid solvents (Figure 5).

All of the lesions examined contained this extensive extracellular lipid deposition; yet the relationship of these droplets to the connective tissue matrix was dependent upon the region of the lipid-rich core being examined. In the center of the lipid-rich core no clear association between the ubiquitous extracellular lipid deposits and specific connective tissue elements could be made. Lipid droplets were found interspersed with collagen, elastin, and reticular ground substance (Figure 6a). In areas of the lipid-rich core with less intense lipid deposition, lipid droplets were found in association with both collagen and elastin (Figure 2a). In some small core regions found primarily in the musculoelastic layer of the intima especially near the core periphery, lipid droplets were present predominantly in association with abundant elastin fibers (Figure 6b). In the lesions with core regions extending upward into the cap region, the lipid droplets were found embedded within collagen bundles (Figure 2c).

Figure 5—Osmium-thiocarbohydrazide-osmium stained fibrolipid lesion. The lipid droplets (*arrows*) are embedded in both collagen and elastin. Note the scalloped appearance of some lipid droplets (*arrowhead*) and the homogeneous nature of the osmiophilic material within the droplets. (No counterstain, bar = 1 μ, ×16,200)

Cholesterol crystallization was observed with three distinct morphologies. Most commonly, cholesterol crystallization was found adjacent to and within elastic fibers (Figure 3a). Cholesterol clefts were also present among bundles of collagen in areas of small lipid droplets surrounded by granular matrix (Figure 3b). Cholesterol crystals were observed within a necrotic cell found near the edge of the lipid-rich core in only one of the 27 specimens examined (Figure 3c). It is interesting to note that the dead cell with intracellular cholesterol clefts had lipid droplets with a distinct scalloped appearance.

Periphery of the Lipid-Rich Core

No clear line of demarcation was found between the lipid-rich core and the surrounding tissue; however, several consistent morphologic features were observed within a broad transition region, which we designated as the core periphery. Near the lateral edges of a core region found in the musculoelastic layer of the intima, the extracellular lipid was still observed in both collagen and elastin fibers (Figure 6a). Where the lipid-rich core made its transition into apparently normal intima, these lipid droplets preferentially localized to elastin fibers despite the presence of collagen (Figure 6b). The luminal boundary of the lipid-rich core region also contained extracellular lipid droplets; however, the droplets were localized primarily to collagen bundles (Figure 7). In this part of the fibrolipid lesion very few elastic fibers were present. The lipid droplets of the core periphery had an appearance similar to that of those observed within the center of the core region. The cells were predominatly SMCs morphologically similar to those found in the core region. Few monocyte-macrophages (Figure 1) were observed at the periphery of most core regions; however, in the large fibrolipid lesions with core regions extending into the elastic hyperplastic layer these cells could be found at the superior and lateral edges of the core.

Stereologic Analyses

The volume compositions of normal intima and of fibrolipid core regions with and without cholesterol crys-

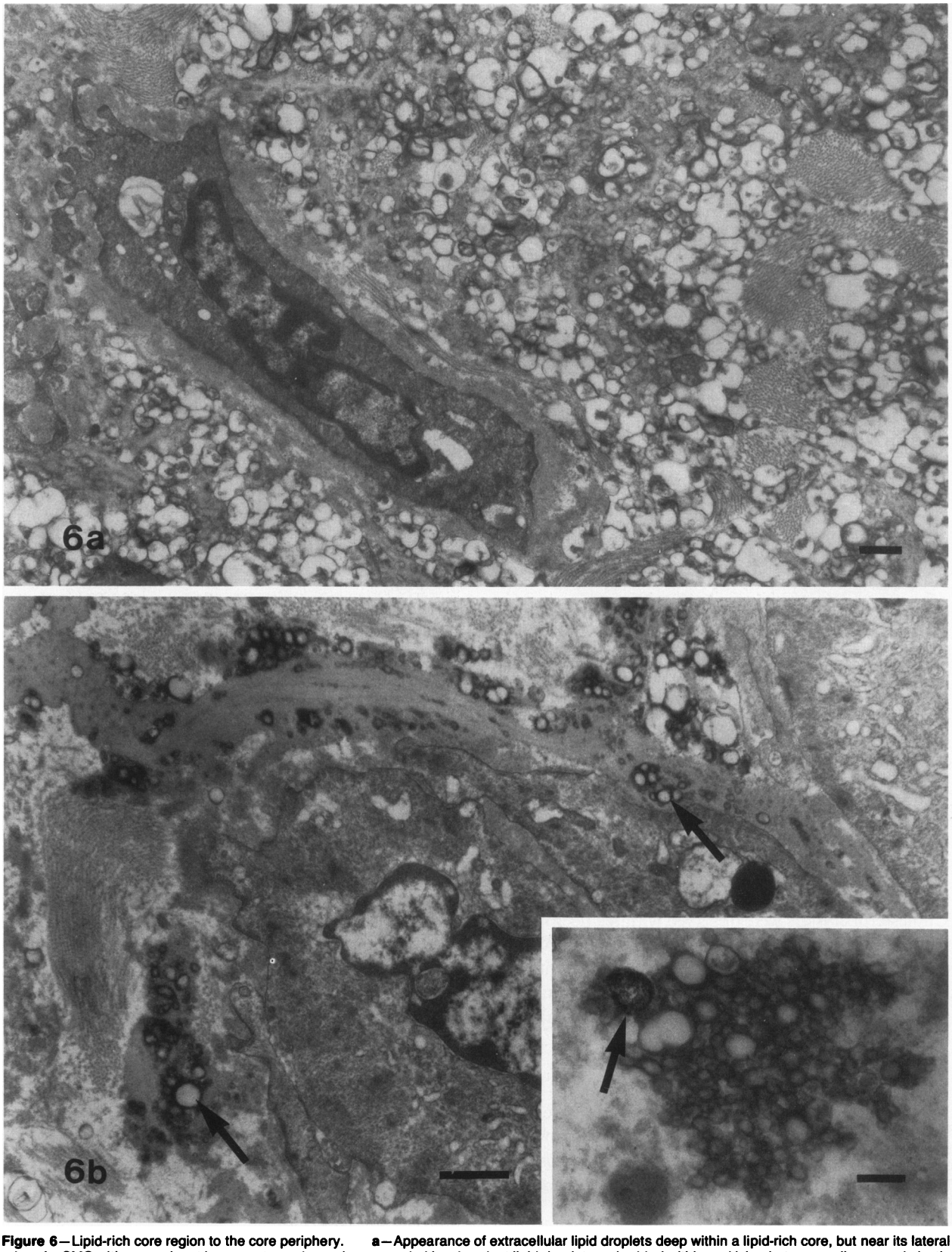

Figure 6—Lipid-rich core region to the core periphery. **a**—Appearance of extracellular lipid droplets deep within a lipid-rich core, but near its lateral edge. An SMC with a prominent basement membrane is surrounded by abundant lipid droplets embedded within and lying between collagen and elastic fibers. (×7650) **b**—Lateral edge of the lipid-rich core. SMCs are present. Lipid droplets (*arrows*) are preferentially localized to elastin, rather than collagen. (×13,050) **Inset**—Higher magnification of small extracellular lipid droplets. The smallest droplet profiles in this group have diameters of approximately 30 nm. Calcific spheroid (*arrow*). (×33,750, bar = 250 nm; uranyl acetate and lead citrate, bars in **a** and **b** = 1 μ)

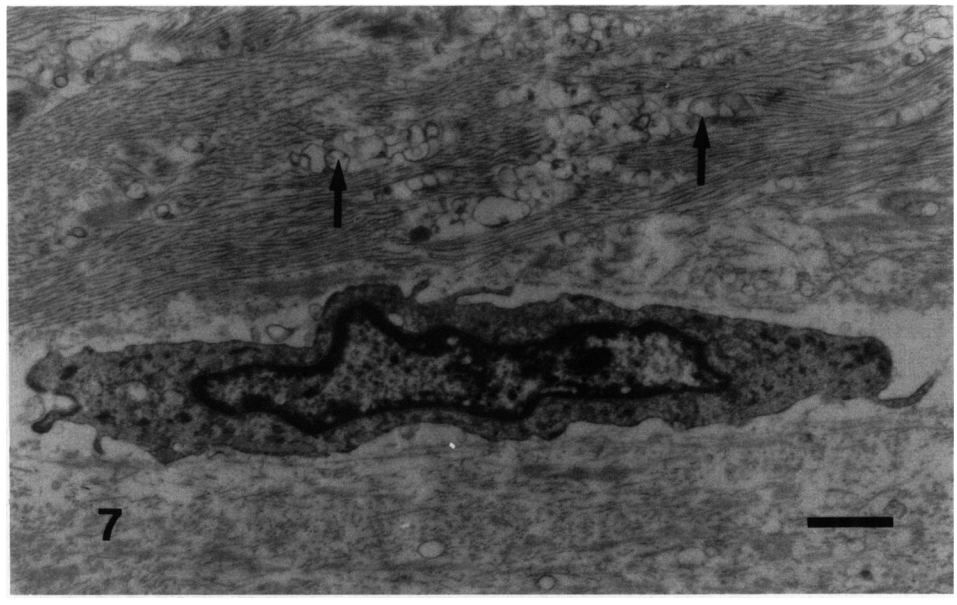

Figure 7—Superficial edge of the lipid-rich core. Lipid (*arrows*) is embedded in collagen bundles. SMCs are present. (Uranyl acetate and lead citrate, bar = 1 μ, ×19,600)

tallization are summarized in Table 1. In normal intima, the 100 μ about the inner limiting membrane contained a total lipid fraction of 4.3%, with 3.5% being extracellular. A 7–10-fold increase in the extent of extracellular lipid was observed in the core regions of fibrolipid lesions with the increase more marked in the lesions with cholesterol crystallization. No significant change in the extent of intracellular lipid was observed, while the volume fraction attributed to cells was significantly reduced ($P < .05$) by 69% and 83% in lesions with and without cholesterol crystals, respectively. In the fibrolipid lesion with cholesterol crystals, the fractions of basement membrane and reticular ground substance were also reduced significantly by 76% and 69%, respectively. A slight reduction in the material identified as elastin in the core region was observed, ie, 17–28%; however, the change was not significant. In this analysis we identified as elastin the granular material surrounding small lipid droplets in the core region (Figure 3a). Although this identification seems likely, it is far from certain, and the possibility of a much greater reduction of elastin in the core region must be considered. The fraction of fibrillar collagen remained constant between normal intima and lesion area.

A profound and highly significant discrepancy between the sizes of intracellular and extracellular droplets can be seen in Figure 8. The mean profile diameter of the extracellular droplets was 0.19 ± 0.11 μ, while the mean of cellular droplets was 1.2 ± 0.43 μ.

Discussion

The present study has provided new electron-microscopic data related principally to the formation of the lipid-rich core region in an early raised atherosclerotic lesion in human aorta. This lesion, which we have termed the fibrolipid lesion, was previously demonstrated to be a progenitor of the fibrous plaque.[1] The

Table 1—Volume Composition of Normal Intima and the Lipid-Rich Core Region of Human Aortic Fibrolipid Lesion

	Normal intima	Fibrolipid lesion without crystals	Fibrolipid lesion with crystals
Number	8	5	7
Fibrillar collagen	0.248 ± 0.105	0.240 ± 0.233	0.253 ± 0.117
Elastin	0.259 ± 0.093	0.214 ± 0.135	0.186 ± 0.102
Basement membrane	0.080 ± 0.027	0.038 ± 0.045	0.019 ± 0.025*
Reticular ground substance	0.193 ± 0.100	0.086 ± 0.075	0.059 ± 0.067*
Cells	0.166 ± 0.098	0.052 ± 0.036*	0.029 ± 0.039*
Extracellular lipid	0.035 ± 0.031	0.322 ± 0.191*	0.440 ± 0.236*
Cellular lipid	0.008 ± 0.020	0.038 ± 0.050	0.003 ± 0.005
Other	0.011	0.010	0.011

Values are the mean ± standard deviation.
* Significantly different from normal intima; $P < 0.05$.

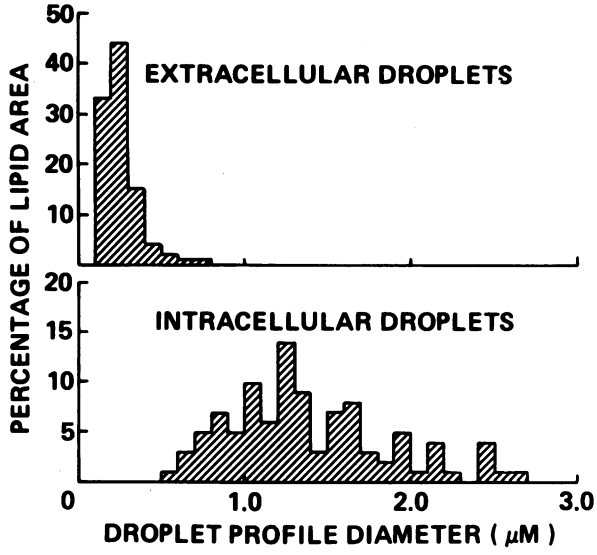

Figure 8—Distribution of lipid according to droplet size.

major implications with regard to the lipid-rich core can be outlined as follows: 1) The abundant extracellular lipid does not appear to arise via foam cell necrosis. 2) Lipid deposition in association with extracellular matrix constituents is an early event in the development of the lipid-rich core.

Near the center of the lipid-rich core, an unbiased sampling procedure revealed that extracellular lipid droplets occupied an average of 32–44% of total volume, depending on the category of fibrolipid lesion. The core region content of cellular lipid was about 10-fold less. This was in contrast to the fibrous cap, where on qualitative observation the lipid was almost entirely cellular, with scant extracellular lipid deposits. A marked size difference was apparent between the cellular and extracellular droplets, with cellular droplet profiles having diameters typically six times larger than the extracellular droplet profiles. Such a size discrepancy suggests that the abundant extracellular lipid may not be the result of cellular necrosis. If that were so, one might expect to find clusters of large lipid droplets in a pattern suggesting sites of foam cell necrosis. However, the patterns of extracellular lipid deposition were either diffuse or clearly associated with extracellular matrix constituents. Unequivocal evidence of foam cell necrosis (Figure 3c) was extremely rare.

An alternative explanation for the discrepancy in lipid droplet sizes would entail a dispersal of lipid contained in a large cellular droplet into smaller droplets shortly after the death of the foam cell. If the process of dispersal were relatively rapid, then transitional forms of lipid would be rare. The scalloped nature of a few larger droplets, seen either extracellularly or in the vicinity of a dead cell, is consistent with this hypothesis. Conceptually, either enzymatic or physicochemical mechanisms could be invoked to explain both the transformation of cholesteryl ester (hydrolysis and/or change of physical state) and the scalloping.[10,11] However, scalloping of a few large droplets must be regarded as scant evidence for the transformation of cellular lipid as a major contributor to the lipid-rich core of the lesion. Moreover, by OTO staining, many smaller extracellular droplets also showed scalloping. Some of these scalloped droplets were embedded within elastic fibers or collagen bundles, where direct deposition of lipid from permeating or bound lipoproteins seemed highly likely. The scalloped appearance of the smaller extracellular droplets could be, of course, an artifact of OTO staining. In routinely prepared specimens this appearance could be neither confirmed nor denied, because of poor preservation of lipid. Overall, the scalloped or cut-out appearance of some lipid droplets is an interesting phenomenon deserving further attention, because it might be a clue to a dynamic state of lipid deposits undergoing continuous deposition and removal.

The selection of small lesions for this study may have been an important factor accentuating the size discrepancy between cellular and extracellular lipid droplets. In the lipid-rich cores of larger fibrous plaques, not fibrolipid lesions, we have observed larger extracellular droplets (not shown). However, we regard the data presented here to be more informative, because the small core regions selected by the present protocol are more likely to be at an early and formative stage of development. The huge extracellular droplets found in some large fibrous plaques could represent an end-stage pathology culminating from years or decades of lesion development with coalescence of lipid. In any case, the present data on lipid droplet sizes mitigate against foam cell necrosis as an event responsible for core *initiation*. Whether the core region may *enlarge* subsequently via foam cell necrosis is a question requiring further study.

The role of cells in lesion development is still unclear. Our previous paper noted and discussed the consistent presence of foam cells in the lesion cap and the relative absence of these cells in the core region.[1] Electron-microscopic examination of the superficial foam cells suggests that most may be derived from monocyte-macrophages, an origin previously suggested by nonspecific acid esterase staining. The presence in the fibrolipid lesion of monocyte-macrophages and SMCs with abundant myofilaments, lipid vacuoles, and rough endoplasmic reticulum is consistent with the notion that the lesion is indeed progressive. The presence of viable-appearing cells within areas of intense extracellular lipid

deposition lends further support to the hypothesis that cell necrosis may not be responsible for the extracellular lipid. This hypothesis contrasts with that of previous investigators,[2-4] who suggested that cell necrosis may be the critical event in lipid-rich core initiation. However, previous studies fail to show sufficient morphologic evidence to support such a hypothesis. It seems possible that cell necrosis may be a secondary consequence of core region development.

A speculative hypothesis for the role of foam cells in lesion development may be that these cells process lipoprotein and lipid, thereby making them more prone to bind to extracellular matrix constituents. For example, the increased ratio of free to esterified cholesterol in the fibrolipid lesion[1] could be due to hydrolysis of cholesteryl ester in cells, with subsequent diffusion and/or transport of individual cholesterol molecules to extracellular binding sites. This speculative scenario would not conflict at all with our findings, since the eventual lipid deposits in the core region would still be assembled extracellularly.

Additional ultrastructural evidence confirms the hypothesis of direct extracellular deposition of the core lipid. We have observed abundant extracellular lipid deposition in the core regions of fibrolipid lesions of all sizes. The lipid was associated intimately with extracellular matrix constituents in the core region. At the periphery of the lipid-rich core, lipid droplets were observed in close association with elastic fibers and collagen bundles. Smith et al[5] and Robertson and coworkers[12] observed at the light-microscopic level that lipid staining along deep elastic membranes was common in normal intima in older subjects. They referred to these lipid deposits as perifibrous lipid. We have recently reported that three-fourths or more of the deep extracellular lipid in normal intima was associated with elastic fibers.[6] Using the OTO *en bloc* staining procedure, we found that the lipid of normal intima was relatively well preserved and more easily visualized. In the present study of fibrolipid lesions, lipid droplets were intensely stained by the OTO procedure and were found associated with both collagen and elastic fibers. The OTO staining adds confirmation that the vesicular structures (by routine staining) associated with collagen and elastin were indeed lipid droplets and not cellular debris.

The idea of direct extracellular deposition of core lipid in atherosclerosis is not new, although ultrastructural evidence previously was lacking. Smith and colleagues[5,13] have shown that the fatty acyl pattern of tissue cholesteryl esters in fibrous plaques is similar to that of plasma low-density lipoproteins. A high fraction of cholesteryl linoleate is found in both. If cell necrosis was the major source of the extracellular lipid, one might expect a tissue fatty acyl pattern similar to that of cellular cholesteryl ester, ie, cholesteryl oleate as the major ester. Kramsch and Hollander[14] and Noma and co-workers[15] have shown that low-density lipoproteins interact strongly with isolated elastin, which results in the uptake of cholesteryl ester by the elastin. It is interesting to note that at the periphery of the lipid-rich core region in the musculoelastic intimal layer, lipid droplets preferentially localized to elastic fibers despite the presence of collagen, basement membrane, and reticular ground substance. Certain proteoglycans of the arterial wall form insoluble complexes with LDL, and this process may disrupt the structural integrity of the LDL particle.[16] Walton and co-workers[17] and Hoff and co-workers[18] have already shown in larger fibrous plaques that the lipid-rich core region contains low-density lipoproteins. We have recently observed that the fibrolipid lesion also contains antigenic determinants reactive with affinity-purified anti-LDL antibodies (unpublished observations). Thus, it seems plausible to hypothesize that an interaction of intimal elastin, collagen, and proteoglycans with permeating lipoproteins could initiate a series of events, yet unknown, that would lead to the formation of the lipid-rich core.

References

1. Bocan TMA, Guyton JR: Human aortic fibrolipid lesions. Progenitor lesions for fibrous plaques, exhibiting early formation of the cholesterol-rich core. Am J Pathol 1985, 120:193–206
2. Geer JC, McGill HC, Strong JP: The fine structure of human atherosclerotic lesions. Am J Pathol 1961, 38:263–287
3. Balis JR, Haust MD, More RH: Electron-microscopic studies in human atherosclerosis: Cellular elements in aortic fatty streaks. Exp Mol Pathol 1964, 3:511–525
4. Haust MD: The morphogenesis and fate of potential and early atherosclerotic lesions in man. Human Pathol 1971, 2:1–29
5. Smith EB, Evans PH, Pownham MD: Lipid in the aortic intima: The correlation of morphological and chemical characteristics. J Atheroscler Res 1967, 7:171–186
6. Guyton JR, Bocan TMA, Schifani TA: A quantitative ultrastructural analysis of perifibrous lipid and its association with elastin in nonatherosclerotic human aorta. Arteriosclerosis 1985, 5:644–652
7. Ross R, Wight TN, Strandness E, Thiele B: Human Atherosclerosis: I. Cell constitution and characteristics of advanced lesions of the superficial femoral artery. Am J Pathol 1984, 114:79–93
8. Willingham MC, Rutherford AV: The use of osmium-thiocarbohydrazide-osmium (OTO) and ferrocyanide-reduced osmium methods to enhance membrane contrast and preservation in cultured cells. J Histochem Cytochem 1984, 32:455–460
9. Wallenstein S, Zucker CL, Fleiss JL: Some statistical methods useful in circulation research. Circulation Res 1980, 47:1–9
10. McGookey DJ, Anderson RGW: Morphological charac-

terization of the cholesteryl ester cycle in cultured mouse macrophage foam cells. J Cell Biol 1983, 97:1156–1168
11. Adams CWM, Abdulla YH: The action of human high density lipoproteins on cholesterol crystals: Part 1. Light-microscopic observations. Atherosclerosis 1978, 31: 465–471
12. Robertson WB, Geer JC, Strong JP, McGill HC, Jr.: The fate of the fatty streak. Exp Mol Pathol 1963, Suppl 1:28–39
13. Smith EB: The relationship between plasma and tissue lipids in human atherosclerosis. Adv Lipid Res 1974, 12: 1–49
14. Kramsch DM, Hollander W: The interaction of serum and arterial lipoproteins with elastin of the arterial intima and its role in the lipid accumulation in atherosclerotic plaques. J Clin Invest 1973, 52:236–247
15. Noma A, Takahashi T, Wada T: Elastin-lipid interaction in the arterial wall: Part 2. In vitro binding of lipoprotein–lipids to arterial elastin and the inhibitory effect of high density lipoproteins on the process. Atherosclerosis 1981, 38:373–382
16. Mateu L, Avila EM, Camejo G, Leon V, Liscano N: The structural stability of low-density lipoprotein. A kinetic X-ray scattering study of its interaction with arterial proteoglycans. Biochim Biophys Acta 1984, 795:525–534
17. Walton KW, Williamson N: Histological and immunofluorescent studies on the evolution of the human atheromatous plaque. J Atheroscler Res 1968, 8:599–624
18. Hoff HF: LDL in the arterial wall: Localization, quantitation, and characterization, Handbook of Electrophoresis. Vol 3. Edited by LA Lewis. Boca Raton, Fla, CRC Press, 1983, pp 133–165